

## Discrete Singular Convolution-Polynomial Chaos Expansion Method for Free Vibration Analysis of Non-uniform Uncertain Beams

Journal:	<i>Journal of Vibration and Control</i>
Manuscript ID	JVC-20-0117.R3
Manuscript Type:	Original Manuscript
Date Submitted by the Author:	21-Oct-2020
Complete List of Authors:	Seçgin, Abdullah; Dokuz Eylul University, Mechanical Engineering Kara, Murat; Bolu Abant Izzet Baysal Universitesi, Mechanical Engineering Ferguson, Neil; University of Southampton,UK
Keywords:	Non-uniform beam, discrete singular convolution, uncertainty, Polynomial Chaos Expansion, natural frequency
Please select up to 5 subject areas that best reflect the content of your manuscript:	Modal analysis, Fundamental dynamics, Modeling, Structural control/vibration mitigation, Analytical methods, Waves in solids and fluids
Abstract:	<p>This paper enhances the Discrete Singular Convolution (DSC) method for free vibration analysis of non-uniform thin beams with variability in their geometrical and material properties such as thickness, specific volume (inverse of density) and Young's modulus. The DSC method solves the differential equation of motion of a structure with a high accuracy using a small number of discretization points. The method utilizes Polynomial Chaos Expansion (PCE) to express these variabilities simulating uncertainty in a closed form. Non-uniformity is locally provided by changing the cross-section and Young's modulus of the beam along its length. In this context, firstly, natural frequencies of deterministic uniform and non-uniform beams are predicted via the DSC. These results are compared with finite element calculations and analytical solutions (if available) for the purpose of verification. Next, the uncertainty of the beam due to geometrical and material variabilities is modelled in a global manner by PCE to predict probability distributed functions of the natural frequencies. Monte Carlo simulations are then performed for validation purpose. Results show that the proposed algorithm of the DSC with PCE is very accurate and also efficient, regarding computation cost, in handling non-uniform beams having material and geometrical variabilities. Therefore it promises that it can be reliably applied to more complex structures having uncertain parameters.</p>

1  
2  
3  
4  
5  
6  
7  
8  
9  
10  
11  
12  
13  
14  
15  
16  
17  
18  
19  
20  
21  
22  
23  
24  
25  
26  
27  
28  
29  
30  
31  
32  
33  
34  
35  
36  
37  
38  
39  
40  
41  
42  
43  
44  
45  
46  
47  
48  
49  
50  
51  
52  
53  
54  
55  
56  
57  
58  
59  
60



# Discrete Singular Convolution-Polynomial Chaos Expansion Method for Free Vibration Analysis of Non-uniform Uncertain Beams

A. Seçgin<sup>a,\*</sup>, M. Kara<sup>b</sup>, N.S. Ferguson<sup>c</sup>

<sup>a</sup> *Department of Mechanical Engineering, Dokuz Eylül University, İzmir, Turkey*

<sup>b</sup> *Department of Mechanical Engineering, Bolu Abant İzzet Baysal University, Bolu, Turkey*

<sup>c</sup> *Institute of Sound and Vibration Research, University of Southampton, Southampton, UK*

*\*Corresponding Author: [abdullah.secgin@deu.edu.tr](mailto:abdullah.secgin@deu.edu.tr)*

**Abstract**— This paper enhances the Discrete Singular Convolution (DSC) method for free vibration analysis of non-uniform thin beams with variability in their geometrical and material properties such as thickness, specific volume (inverse of density) and Young's modulus. The DSC method solves the differential equation of motion of a structure with a high accuracy using a small number of discretization points. The method utilizes Polynomial Chaos Expansion (PCE) to express these variabilities simulating uncertainty in a closed form. Non-uniformity is locally provided by changing the cross-section and Young's modulus of the beam along its length. In this context, firstly, natural frequencies of deterministic uniform and non-uniform beams are predicted via the DSC. These results are compared with finite element calculations and analytical solutions (if available) for the purpose of verification. Next, the uncertainty of the beam due to geometrical and material variabilities is modelled in a global manner by PCE to predict probability distributed functions of the natural frequencies. Monte Carlo simulations are then performed for validation purpose. Results show that the proposed algorithm of the DSC with PCE is very accurate and also efficient, regarding computation cost, in handling non-uniform beams having material and geometrical variabilities. Therefore it promises that it can be reliably applied to more complex structures having uncertain parameters.

**Keywords**— Non-uniform beam, discrete singular convolution, uncertainty, Polynomial Chaos Expansion

## 1. Introduction

In engineering, structures generally have different geometrical shapes and sometimes they are non-uniform along the structure for engineering reasons. Non-uniformity is generally provided to reinforce the regions with different stress distributions, especially for beams which are one of the most commonly used engineering structures. It is generally accomplished by changing either the mechanical or geometrical properties in a local manner along the structure. These types of structures are called as Functionally Graded Materials (FGMs) in literature (Akgöz and Civalek, 2013; Alshorbagy et al., 2011; Sankar, 2001). However, the same structures or components manufactured by the same mass production line may exhibit different dynamic characteristics for an unpredicted reason. These variabilities are generally labelled as uncertainty. Uncertainty and variability are unavoidable, due to various reasons such as material heterogeneity, production tolerances, manufacturing defects, environmental factors, etc. A good example for variability is a work of Kompella and Bernhard (1993). Structure-borne sound at the driver position in 57 samples of Isuzu pick-up trucks, were produced in the same production line, clearly showed variability. Many experiments and practical cases in industry showed that for a realistic design, uncertainty needs to be taken into account starting in the product design stage. Besides, it is also observed that higher frequencies are much more sensitive to these variabilities. This requirement leads to the development of some simulation methods for quantifying these variabilities. Methods used in uncertainty analysis may be categorized as probabilistic and non-probabilistic methods. Non-probabilistic methods are used in cases where the statistical properties of uncertain parameters are not known, but the limits of them are known. In such methods, only the limits of the uncertain response variable are obtained. When statistics of uncertain parameters are known or properly assumed, probabilistic methods such as Monte Carlo simulation (Evans and Swartz, 2000; Rubinstein and Kroese, 2016), first and second order

1  
2  
3 reliability methods (Hohenbichler and Rackwitz, 1989; Keane and Price, 1997), numerical  
4 integration based methods (Evans, 1972; Rahman and Xu, 2004; Seo and Kwak, 2002) and  
5 spectral methods (Ghanem and Spanos, 2003; Lucor et al., 2004; Sepahvand, 2017;  
6 Sepahvand et al., 2007, 2010) can be appropriate methodologies to be selected. Among them,  
7 Monte Carlo simulations are the most widely used technique. However, it requires significant  
8 numerous experiments/simulation sets in order to determine response statistics, which makes  
9 it inefficient. Recently, spectral methods like Karhunen-Loeve (KL) (Ghanem and Spanos,  
10 2003) or Polynomial Chaos Expansion (PCE) (Lucor et al., 2004; Sepahvand, 2017;  
11 Sepahvand et al., 2007, 2010), are preferable amongst the researchers since the variability is  
12 defined in a set of closed form equations.

13  
14  
15  
16  
17  
18  
19  
20  
21  
22  
23  
24  
25  
26 Beams are one of the most basic and thus most attracted structural element in the research  
27 studies for the test and validation purpose of newly developed methods (Bailey, 1978;  
28 Elishakoff and Johnson, 2005; Korayem et al., 2012; Korayem and Homayooni, 2017; Wei,  
29 2001b, 2001c; Wei et al., 2002a). For example, Bailey (1978) developed a direct analytical  
30 solution, Elishakoff and Johnson (2005) introduced a closed form solution procedure and all  
31 of them tested their techniques on non-uniform beams. Tan et. al. (2016, 2018) demonstrated  
32 approaches for the free vibrations of cracked and non-cracked non-uniform beams.  
33 Nazemizadeh and Bakhtiari-Nejad (2015) investigated the quality factor of composite  
34 micro/nano beams employing the nonlocal Euler-Bernoulli beam theory. Similarly, Wei  
35 (2001b, 2001c; 2002a) also tested his numerical approach, Discrete Singular Convolution  
36 (DSC), on uniform bars and beams in his early studies.

37  
38  
39  
40  
41  
42  
43  
44  
45  
46  
47  
48  
49  
50  
51 The DSC method (Wei, 1999) promises great potential especially in handling high  
52 frequency structural dynamic problems. Because it has inherent global method accuracy and  
53 local method flexibility together with requiring a small number of discretization points to  
54 define the geometrical domain. The method is based on the theory of distributions and  
55  
56  
57  
58  
59  
60

1  
2  
3 wavelets. The DSC method solves the governing differential equation of motion of a structure  
4 with a high accuracy using a small number of discretization points. Wei and his co-workers  
5 applied the DSC method to several different vibration problems (Wei, 2001a, 2001b, 2001c;  
6 Wei et al., 2001, 2002a, 2002b; Zhao et al., 2005). Seçgin and Sarigül (2008) adapted the  
7 DSC method to analyse vibration problems of laminated composite plates. Similarly, Civalek  
8 et. al. (Baltacıoğlu et al., 2010, 2011; Civalek, 2007, 2013; Gürses et al., 2009) have made  
9 great contribution to the development of the DSC, especially for the analysis of laminated  
10 plates and nano-structures (Civalek, 2017; Gürses et al., 2012; Mercan and Civalek, 2016).  
11 Beside that, Shokrollahi et. at. (2014) investigated the natural frequencies of non-uniform bars  
12 having different combinations of cross-sections via the DSC. Civalek et. al. (2008a, 2008b,  
13 2009; Ersoy et al., 2009, 2010) applied the DSC to more complex non-uniform structures, i.e.,  
14 shell and membranes. Seçgin (2013; 2012; 2018) also combined the DSC with some  
15 uncertainty analysis methods. He performed Monte Carlo simulation by using the DSC for a  
16 thin isotropic plate and laminated composite plates in Refs. (Seçgin, 2013; Seçgin et al.,  
17 2012), respectively, in order to estimate the statistical bounds of vibration via an extreme  
18 value model. In another study, Seçgin and Kara (2018) developed a closed form solution  
19 methodology for the analysis of uncertain thin beams. In that study, they showed that the DSC  
20 presents a unique advantage since the characteristic matrix obtained via the DSC is  
21 independent from physical and mechanical properties of the considered structure. Besides, the  
22 DSC method is very efficient for the higher frequencies where the uncertainty dominates,  
23 since the method uses a relatively small number of discretization points.

24  
25  
26  
27  
28  
29  
30  
31  
32  
33  
34  
35  
36  
37  
38  
39  
40  
41  
42  
43  
44  
45  
46  
47  
48  
49  
50  
51  
52  
53  
54  
55  
56  
57  
58  
59  
60

As far as to the authors' knowledge, there are limited number of studies on uncertain and non-uniform structures in literature (2004; 2003). Impollonia and his/her colleagues (2004; 2003) analysed static response of uncertain tapered cantilever beams via a novel response surface approach. Besides, there is no attempt yet to show the performance of the combined

1  
2  
3 DSC and PCE for both uncertain and non-uniform structures. Therefore, this study performs  
4 such an attempt to test the methodology and applies the DSC method for more sophisticated  
5 structures.  
6  
7  
8  
9

10 In this study, the Discrete Singular Convolution (DSC) and Polynomial Chaos Expansion  
11 PCE are combined in order to analyse uncertain non-uniform beams. Non-uniformity is  
12 locally provided by a changing cross-section and Young's modulus of the beam along its  
13 length. However, the uncertainty is globally simulated by providing normally distributed  
14 variabilities in geometrical and material properties such as thickness, specific volume and  
15 Young's modulus. Here, the non-uniform beam is modelled via the DSC whereas uncertainty  
16 is defined by PCE in a closed form. In this context, the implementation procedure of the DSC  
17 and PCE is given in detail. Numerical analyses start with the prediction of the natural  
18 frequencies of deterministic uniform and non-uniform beams via the DSC. The results are  
19 verified by finite element calculations and analytical solutions (if possible). Then, the  
20 uncertainty of the beam due to geometrical and material variabilities is considered, and  
21 probability distribution functions of natural frequencies are determined by the DSC-PCE  
22 combination. Monte Carlo simulations are then performed for validation purpose. It is shown  
23 that the DSC-PCE combination is very accurate as well as being efficient regarding  
24 computation cost.  
25  
26  
27  
28  
29  
30  
31  
32  
33  
34  
35  
36  
37  
38  
39  
40  
41  
42  
43  
44  
45  
46

## 47 **2. Mathematical Considerations**

### 48 ***2.1. Stochastic partial differential equation of non-uniform thin beams***

49  
50  
51 The homogeneous differential equation of motion for bending vibrations of an undamped  
52 thin beam (shown in Fig. 1) with variable thickness and Young's modulus along space is  
53 expressed as follows (Rao, 2011):  
54  
55  
56  
57  
58  
59  
60

$$\frac{\partial^2}{\partial x^2} \left( E(x) I_y(x) \frac{\partial^2 w(x,t)}{\partial x^2} \right) + \rho A(x) \frac{\partial^2 w(x,t)}{\partial t^2} = 0. \quad (1)$$

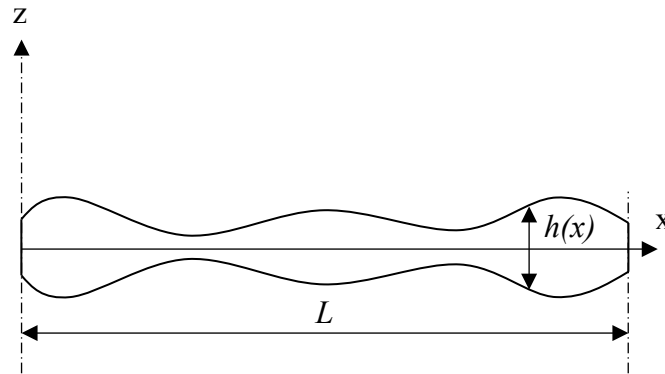


Figure 1. A beam structure with its geometrical parameters

Here,  $x$  is the space variable,  $\rho$  is uniform mass density,  $w$  is the bending displacement in the  $z$  direction,  $E(x)$ ,  $h(x)$ ,  $A(x)$  and  $I_y(x)$  are the space dependent Young's modulus, thickness, cross-sectional area and area moment of inertia about the  $y$  axis, respectively. Assume that the beam has constant width  $b$ , the thickness and Young's modulus have the form of  $h(x) = h_0 f_h(x)$  and  $E(x) = E f_E(x)$  where  $h_0$  and  $E$  are the thickness and Young's modulus at  $x=0$ ,  $f_h(x)$  and  $f_E(x)$  represent the space dependency of thickness and the Young's modulus, respectively. In this context, the separable solution of Eq. (1) can be rewritten for harmonic free vibration response  $w(x,t,\vartheta) = W(x,\vartheta) \exp(j\omega_n t)$  with stochastic parameters  $\vartheta = \{\vartheta_1, \vartheta_2, \vartheta_3\}$  ( $W$  is time independent stochastic vibration amplitude,  $\omega_n$  is the natural frequency,  $\vartheta_1$ ,  $\vartheta_2$ ,  $\vartheta_3$  are the uncertain parameters affecting Young's modulus, thickness and density, respectively and  $j = \sqrt{-1}$ ) as follows,

$$\begin{aligned} & \frac{1}{12} E(\vartheta_1) h_0^2(\vartheta_2) r(x, \vartheta_3) \left[ f_E f_h^2 W^{(4)}(x, \vartheta) + 2 \left( f_E^{(1)} f_h^2 + 3 f_E f_h^{(1)} f_h \right) W^{(3)}(x, \vartheta) \right. \\ & \left. + \left( f_E^{(2)} f_h^2 + 6 f_E^{(1)} f_h^{(1)} f_h + 6 f_E \left( f_h^{(1)} \right)^2 + 3 f_E f_h^{(2)} f_h \right) W^{(2)}(x, \vartheta) \right] - \lambda_n(\vartheta) W(x, \vartheta) = 0. \end{aligned} \quad (2)$$



Here  $r(x, \vartheta_3) = 1/\rho(x, \vartheta_3)$  is defined as the specific volume. The superscripts in parenthesis shows the order of differentiation with respect to space  $x$ , and  $\lambda_n = \omega_n^2$  is the eigenvalue of the structure.

## 2.2. Discrete Singular Convolution

In the DSC algorithm, the computational domain of a 1D system is generally divided into three different parts; structural, left and right ghost (auxiliary) domains as shown in Fig. 2. In the computational domain, a function  $f(x)$  and its  $n$ th order derivative can be approximated via a discretized singular kernels of delta type (Wei, 2001c):

$$f^{(n)}(x_i) \approx \sum_{k=-M}^M C_k^{(n)} f(x_{i+k}), \quad i = 0, 1, 2, \dots, M \quad (3)$$

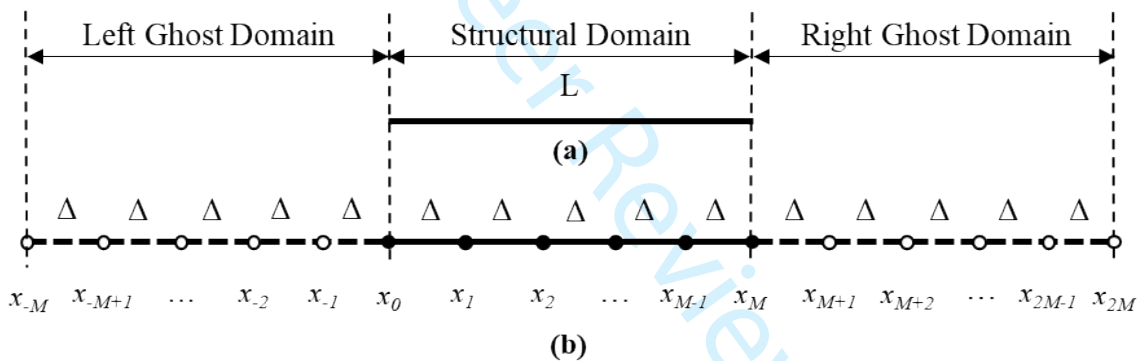


**Figure 2. DSC discretization domain for 1-D structures (a) a 1D structure with length L, (b) Computational domain for the structure (Seçgin and Sarigül, 2008)**

Here,  $i$  represents the index of discretization points in the structural domain and  $M$  stands for the number of ghost points. The function  $f(x)$  is determined at uniformly distributed discretization points. The term  $C_k^{(n)}$  is the DSC kernel and can be expressed for regularized Shannon delta kernel as (Wei, 2001c):

$$C_k^{(n)} = \left( \frac{d}{dx} \right)^n \left( \frac{\sin(\alpha(x-x_k))}{\alpha(x-x_k)} \exp\left(-\frac{(x-x_k)^2}{2\sigma^2}\right) \right) \Bigg|_{x=x_i}, \quad (4)$$

where  $\alpha = \pi/\Delta$  is Nyquist frequency,  $\sigma = r\Delta$ ,  $\Delta$  represents the distance between the discretization points and  $r$  is regularization coefficient which can be selected by trial and error to confirm accuracy, and superscript  $n$  stands for the order of the derivative. One can follow the following steps in order to model a beam structure via the DSC:

1. The beam is discretized by using  $M+1$  number of structural and  $M$  number of ghost points as shown in Fig. 2.
2. Eq. (3) is written for each structural point.
3. Kernel coefficients  $C_k^{(n)}$  are computed from Eq. (4)
4. Proper boundary condition implementation procedure is performed to get rid of the displacement in the ghost domains. Note that, this procedure is given in detail in Ref. (Kara and Seçgin, 2019; Seçgin and Sarigül, 2008, 2009) for clamped, simply supported and free boundary conditions.
5. Next, Eq. (3) can be written in a matrix form as an eigenvalue problem,

$$\left( E(\vartheta_1)h^2(\vartheta_2)r(\vartheta_3)[\mathbf{D}(\mathbf{X})] - \lambda_n(\vartheta)[\mathbf{I}] \right) \{ \mathbf{W}(\mathbf{X}, \vartheta) \} = 0 . \quad (5)$$

Here,  $[\mathbf{D}(\mathbf{X})]$  is the dynamic stiffness matrix,  $\mathbf{X} = \{X_0, X_1, \dots, X_M\}^T$  represents the vector for the discretized structural points and  $\mathbf{W} = \{W_0, W_1, \dots, W_M\}^T$  is the corresponding bending displacement vector for the structural points. It should be noted that, the dynamic stiffness matrix is independent from the amplitude of physical and mechanical properties ( $E$ ,  $h_0$  and  $r$ ). Thus, in the DSC, once the matrix is calculated, one may then calculate the dynamic response and/or eigenvalues for different materials and thicknesses. To show the content of the dynamic stiffness matrix, the  $i$ th row of the matrix which belongs to  $(i-1)$ th structural point is given here as:

$$\begin{aligned} \{\mathbf{D}(\mathbf{X})\}_{1 \times (M+1)} &= \frac{1}{12} (f_E f_h^2) \Big|_{x=X_{i-1}} \{\mathbf{D}^{(4)}\} + \frac{1}{6} (f_E^{(1)} f_h^2 + 3f_E f_h^{(1)} f_h) \Big|_{x=X_{i-1}} \{\mathbf{D}^{(3)}\} \\ &+ \frac{1}{12} (f_E^{(2)} f_h^2 + 6f_E^{(1)} f_h^{(1)} f_h + 6f_E (f_h^{(1)})^2 + 3f_E f_h^{(2)} f_h) \Big|_{x=X_{i-1}} \{\mathbf{D}^{(2)}\} \end{aligned} \quad (6)$$

Here,  $\{\mathbf{D}^{(n)}\}$  is the  $i$ th row of the characteristic DSC matrix of differentiation order of  $n$ . Note that, space dependent functions and their derivatives are calculated at  $x=X_{i-1}$ .

### 2.3. Polynomial Chaos Expansion (PCE)

In Polynomial Chaos Expansion (PCE), any uncertain variable  $Y$  can be expressed as the sum of orthogonal polynomials (Ghanem and Spanos, 2003):

$$\begin{aligned} Y(\xi) &= y_0 \psi_0 + \sum_{i_1=1}^{\infty} y_{i_1} \psi_1(\xi_{i_1}) + \sum_{i_1=1}^{\infty} \sum_{i_2=1}^{i_1} y_{i_1 i_2} \psi_2(\xi_{i_1}, \xi_{i_2}) + \sum_{i_1=1}^{\infty} \sum_{i_2=1}^{i_1} \sum_{i_3=1}^{i_2} y_{i_1 i_2 i_3} \psi_3(\xi_{i_1}, \xi_{i_2}, \xi_{i_3}) + \dots \\ &= \sum_{i=0}^{\infty} y_i \psi_i(\xi) \end{aligned} \quad (7)$$

Here,  $\xi = \{\xi_1, \xi_2, \dots, \xi_n\}$  is the vector containing stochastic parameters,  $y_i$  is deterministic coefficients of orthogonal polynomial basis of  $\psi_i(\cdot)$ . Since polynomial terms are orthogonal to each other;

$$\langle \psi_i \cdot \psi_j \rangle = \begin{cases} 0, & \text{for } i \neq j \\ \langle \psi_i^2 \rangle, & \text{for } i = j \end{cases} \quad (8)$$

Here,  $\langle \cdot \rangle$  represents the mean value. In numerical calculations, it is meaningful to cease infinite series the sum of the polynomial in Eq. (7) by a finite value of terms  $N_{PC}$  (Sepahvand et al., 2010):

$$N_{PC} = \frac{(m+p)!}{m!p!} - 1 \quad (9)$$

Here,  $p$  shows the order of polynomial,  $m$  shows number of uncertain parameter ( $\xi_i$ ) to define uncertain variable ( $Y$ ). In PCE, unknown deterministic coefficients of the polynomials can be

determined by using a Galerkin projection which may be described as calculating the average of the considered equation and basis polynomial function multiplication (Sepahvand et al., 2010):

$$y_i = \frac{1}{\langle \psi_i^2 \rangle} \int_{\Omega} \dots \int_{\Omega_m} \langle Y, \psi_k(\xi) \rangle d\mu_m(\xi_m) \dots d\mu_1(\xi_1). \quad (10)$$

Note that,  $d\mu(\xi) = \mu(\xi)d\xi$  is the probability function of the random space ( $\Omega$ ) of uncertain parameter ( $\xi$ ) and  $k$  is an integer starting from zero. Several types of polynomial basis functions ( $\psi_i$ ) such as Laguerre polynomial, Jacobi polynomial, Legendre polynomial, etc. can be used in PCE, but Hermite polynomials are the most suitable one for the normal distribution (Ghanem and Spanos, 2003):

$$H_i(\xi) = (-1)^i \exp\left(\frac{1}{2}\xi^T \xi\right) \frac{\partial^i}{\partial \xi_{i_1} \partial \xi_{i_2} \dots \partial \xi_{i_n}} \exp\left(-\frac{1}{2}\xi^T \xi\right). \quad (11)$$

In PCE, using a first order polynomial is sufficient for representation of a normal distribution with Hermite polynomials with a single uncertain parameter, so PCE then reduces to Karhunen-Loève (KL) expansion ( $N_{PC} = 1$ ).

In this study, stochastic parameters given in Section 2.1 can be redefined as  $\mathfrak{G}_i = \{\xi_{i,1}, \xi_{i,2}, \dots, \xi_{i,n}\}$ . It is assumed that all uncertain variables depend on a single uncertain variable ( $\mathfrak{G}_i = \xi_{i,1} = \xi_i$ ) with a normal distribution. Therefore uncertain variables can be rewritten as follows:

$$E(\mathfrak{G}_1) = \sum_{i=0}^1 E_i H_i(\xi_1) = E_0 + E_1 \xi_1, \quad (12)$$

$$h^2(\mathfrak{G}_2) = \sum_{j=0}^1 h_j^2 H_j(\xi_2) = h_0^2 + h_1^2 \xi_2, \quad (13)$$

$$r(\vartheta_3) = \sum_{k=0}^1 r_k H_k(\xi_3) = r_0 + r_1 \xi_3. \quad (14)$$

Note that,  $E_0$ ,  $h_0$  and  $r_0$  are the mean values of the Young's modulus and thickness at  $x=0$ , and specific volume, respectively.  $E_1$ ,  $h_1$  and  $r_1$  are the standard deviations of those uncertain parameters. Eqs. (12)-(14) can be written in the vector form as:

$$E(\vartheta_1) = \{E_0 \quad E_1\} \begin{Bmatrix} 1 \\ \xi_1 \end{Bmatrix}, \quad (15)$$

$$h^2(\vartheta_2) = \{h_0^2 \quad h_1^2\} \begin{Bmatrix} 1 \\ \xi_2 \end{Bmatrix}, \quad (16)$$

$$r(\vartheta_3) = \{r_0 \quad r_1\} \begin{Bmatrix} 1 \\ \xi_3 \end{Bmatrix}. \quad (17)$$

Polynomial basis terms of the corresponding eigenvalues are written by using the tensor product of Eqs. (15)-(17);

$$\psi_k(\xi_1, \xi_2, \xi_3) = \begin{Bmatrix} 1 \\ \xi_1 \end{Bmatrix} \otimes \begin{Bmatrix} 1 \\ \xi_2 \end{Bmatrix} \otimes \begin{Bmatrix} 1 \\ \xi_3 \end{Bmatrix}. \quad (18)$$

Here,  $\otimes$  denotes the tensor product. Since the dimension of the vector  $\psi_k(\xi_1, \xi_2, \xi_3)$  is  $8 \times 1$ , the uncertain eigenvalues are described by the summation starting from 0 to  $N_\lambda = 7$  as follows,

$$\begin{aligned} \lambda_n &= \sum_{k=0}^{N_\lambda} \lambda_{n,k} \psi_k(\xi_1, \xi_2, \xi_3) \\ &= \lambda_{n,0} + \lambda_{n,1} \xi_1 + \lambda_{n,3} \xi_2 + \lambda_{n,4} \xi_3 + \lambda_{n,4} \xi_1 \xi_2 + \lambda_{n,5} \xi_1 \xi_3 + \lambda_{n,6} \xi_2 \xi_3 + \lambda_{n,7} \xi_1 \xi_2 \xi_3 \end{aligned} \quad (19)$$

Substituting Eqs. (12)-(14) and Eq. (19) into Eq. (5) leads to:

$$\left[ (E_0 + E_1 \xi_1) (h_0^2 + h_1^2 \xi_2) (r_0 + r_1 \xi_3) \mathbf{D}(\mathbf{X}) - \lambda_n(\xi_1, \xi_2, \xi_3) \mathbf{I} \right] \{ \mathbf{W}(\mathbf{X}, \vartheta) \} = 0. \quad (20)$$

Multiplying Eq. (20) with the  $u$ th term of the orthogonal basis of  $\psi_k$  and applying the Galerkin projection yields the final form of DSC-PCE based eigenvalue equation of a non-uniform and uncertain thin beam:

$$\left( \begin{array}{l} (E_0 + E_1 \xi_1)(h_0^2 + h_1^2 \xi_2)(r_0 + r_1 \xi_3) \psi_u(\xi_1, \xi_2, \xi_3) \mathbf{D}(\mathbf{X}) \\ - \lambda_{n,u} \psi_u^2(\xi_1, \xi_2, \xi_3) \mathbf{I} \end{array} \right) \{ \mathbf{W}(\mathbf{X}, \mathfrak{g}) \} = 0 \quad (21)$$

One can now calculate  $\lambda_{n,u}$  by changing  $u$  starting from zero up to  $N_\lambda$  in Eq. (21) by using any eigenvalue solver.

### 3. Numerical studies

In this section, free vibration analyses of a non-uniform and uncertain thin beam with simply-supported boundary conditions are performed. Material and geometrical properties of the beam are given in Table 1. The study starts with a deterministic analysis for uniform and non-uniform beams. Then, stochastic analyses are performed for the non-uniform beam with variable material and geometrical properties by using the PCE based DSC method. Both studies include a verification and convergence investigation. Numerical analyses are performed by a computer with Intel Core i5-3230M 4x2.6 GHz, 8 GB Ram, 64 Bit Win 10.

**Table 1. Material and geometrical properties of the beam**

Property (Unit)	Value
Young' modulus (Pa)	3.25E+10
Density (kgm <sup>-3</sup> )	2500
Thickness at $x=0$ (m)	0.25
Width (m)	0.3
Length (m)	15

### 3.1. Deterministic analysis

Here, firstly a uniform beam is considered. The first ten natural frequencies are obtained via the DSC method for different numbers of structural points and via the finite element method (FEM) for different numbers of one dimensional beam elements. The results are compared with analytical solutions in Table 2 and an optimum number of structural points for the DSC and number of elements for FEM are determined for further analyses. In this regard, relative differences of the DSC and FEM from analytical solutions are also presented in the table. The thickness is selected as 0.25 m in these calculations. Note that the maximum number of the DSC points and finite elements are decided here to achieve the same analytical results in a 3-digit-floating accuracy.

**Table 2. Natural frequencies of the simply supported uniform beam (rad/s)**

Mode Seq.	Analy. (Rao, 2011)	DSC N=11	DSC N=21	DSC N=31	FEM N=20	FEM N=60	FEM N=120	FEM N=230
1	11.414	11.411	11.414	11.414	11.414	11.414	11.414	11.414
2	45.656	45.667	45.656	45.656	45.656	45.656	45.656	45.656
3	102.726	102.828	102.726	102.726	102.730	102.726	102.726	102.726
4	182.624	183.501	182.624	182.624	182.644	182.624	182.624	182.624
5	285.350	290.841	285.350	285.350	285.424	285.351	285.350	285.350
6	410.904	434.686	410.904	410.904	411.124	410.907	410.905	410.904
7	559.287	627.888	559.287	559.287	559.835	559.294	559.287	559.287
8	730.497	858.099	730.497	730.497	731.707	730.512	730.498	730.497
9	924.535	1059.665	924.538	924.535	926.960	924.566	924.537	924.535
10	1141.401		1141.427	1141.401	1145.906	1141.460	1141.405	1141.401
<b>Error %</b>								
1	-	-2.78E-02	-3.55E-05	-4.39E-07	4.22E-05	4.92E-07	2.80E-06	8.27E-06
2	-	2.35E-02	2.16E-06	2.71E-08	6.75E-04	8.35E-06	5.94E-07	1.01E-06
3	-	9.94E-02	-4.05E-07	-5.27E-09	3.40E-03	4.22E-05	2.70E-06	5.67E-07
4	-	4.80E-01	1.20E-07	1.62E-09	1.07E-02	1.33E-04	8.36E-06	8.20E-07
5	-	1.92E+00	-2.74E-08	-6.42E-10	2.60E-02	3.26E-04	2.04E-05	1.61E-06
6	-	5.79E+00	2.57E-07	2.98E-10	5.34E-02	6.75E-04	4.22E-05	3.14E-06
7	-	1.23E+01	3.01E-06	-1.51E-10	9.81E-02	1.25E-03	7.83E-05	5.82E-06
8	-	1.75E+01	3.26E-05	8.31E-11	1.66E-01	2.13E-03	1.33E-04	9.90E-06
9	-	1.46E+01	2.97E-04	-4.72E-11	2.62E-01	3.40E-03	2.14E-04	1.59E-05
10	-		2.24E-03	2.80E-11	3.95E-01	5.18E-03	3.26E-04	2.42E-05

1  
2  
3 It is seen from Table 2 that the DSC accurately predicts the same analytical results, while  
4 FEM achieves the same accuracy with 230 elements. For this discretization points and  
5 number of elements, maximum relative differences are  $-4.39\text{E-}07$  and  $2.42\text{E-}05$  for the DSC  
6 and FEM, respectively. Therefore,  $M+1=31$  for the DSC and  $N=230$  for the FEM are selected  
7 in the further analyses.  
8  
9  
10  
11  
12  
13  
14  
15  
16

17 Next, analysis of a non-uniform beam (the beam with variable geometry and material  
18 properties along its length) is performed. Again ten natural frequencies were determined for i)  
19 the beam with non-uniform thickness, ii) the beam with non-uniform Young's modulus and  
20 iii) the beam with non-uniform thickness and Young's modulus. In the analyses, two different  
21 forms of the spatial variations are assumed for the thickness i.e,  $h_0 f_h(x) = h_0(1 + \beta x)^2$  and  
22  $h_0 f_h(x) = h_0(1 + \beta x)$  (non-uniformity parameter of thickness constant  $\beta$  is selected as  
23  $-0.0109$ ) and for Young's modulus i.e,  $E f_E(x) = E(1 + 0.02 \cos(2\pi x/l) + 0.01 \sin(4\pi x/l))$   
24 and  $E f_E(x) = E(1 - 0.02 x/l)^2$ . Spatial variations of non-uniformities are plotted in Fig. 3 and  
25 the natural frequency computations are tabulated in Table 3 together with the relative  
26 difference %.  
27  
28  
29  
30  
31  
32  
33  
34  
35  
36  
37  
38  
39  
40  
41  
42  
43  
44  
45  
46  
47  
48  
49  
50  
51  
52  
53  
54  
55  
56  
57  
58  
59  
60



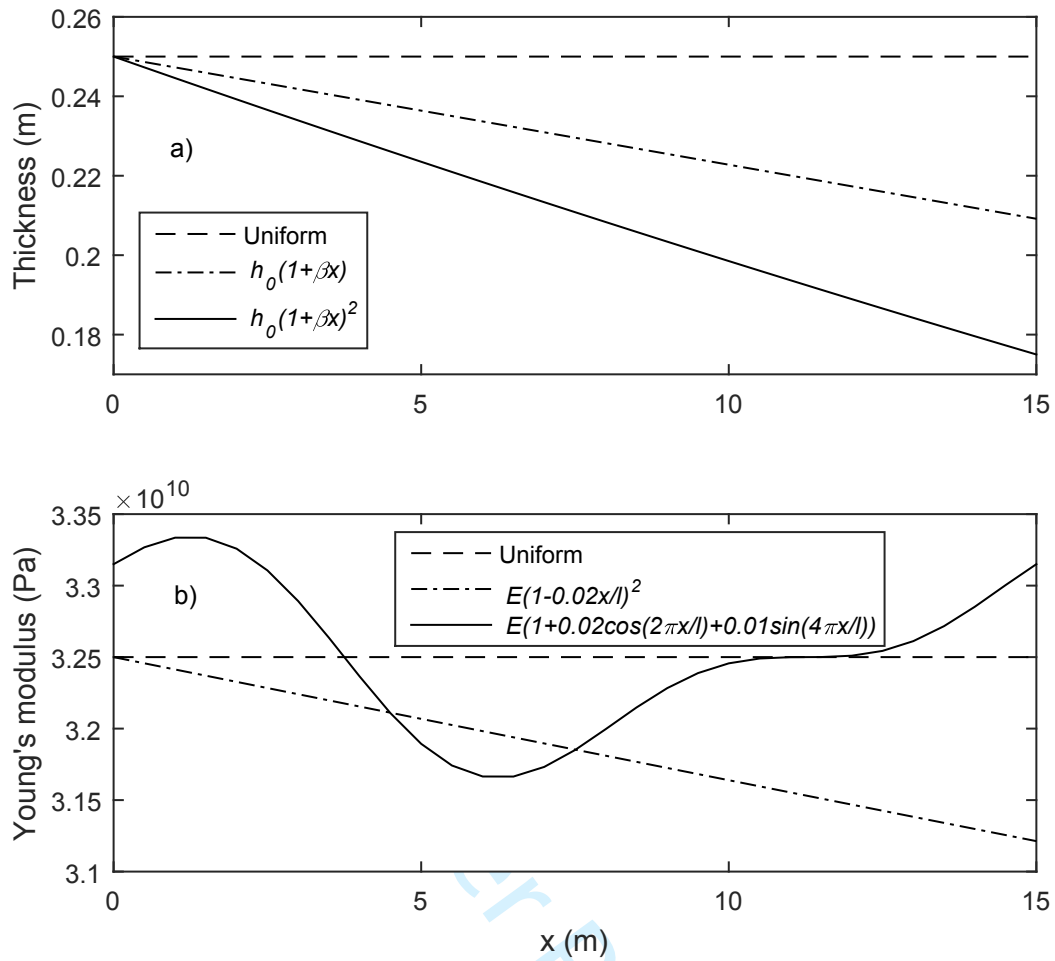


**Figure 3. The spatial variations of non-homogeneities a) thickness, b) Young modulus**

1  
2  
3  
4  
5  
6  
7  
8  
9  
10  
11  
12  
13  
14  
15  
16  
17  
18  
19  
20  
21  
22  
23  
24  
25  
26  
27  
28  
29  
30  
31  
32  
33  
34  
35  
36  
37  
38  
39  
40  
41  
42  
43  
44  
45  
46

**Table 3. Natural frequencies of the simply supported non-uniform beam (rad/s)**

Form of thickness and Young's modulus	$h(x) = h_0(1 + \beta x)^2$ $E(x) = E$			$h(x) = h_0$ $E(x) = E \begin{pmatrix} 1 + 0.02 \cos(2\pi x/l) \\ +0.01 \sin(4\pi x/l) \end{pmatrix}$			$h(x) = h_0(1 + \beta x)^2$ $E(x) = E \begin{pmatrix} 1 + 0.02 \cos(2\pi x/l) \\ +0.01 \sin(4\pi x/l) \end{pmatrix}$			$h(x) = h_0(1 + \beta x)$ $E(x) = E \begin{pmatrix} 1 + 0.02 \cos(2\pi x/l) \\ +0.01 \sin(4\pi x/l) \end{pmatrix}$			$h(x) = h_0(1 + \beta x)^2$ $E(x) = E(1 - 0.02 x/l)^2$			$h(x) = h_0(1 + \beta x)$ $E(x) = E(1 - 0.02 x/l)^2$		
	Mode Seq.	DSC M+1=31	FEM N=230	Rel. Diff. %	DSC M+1=31	FEM N=230	Rel. Diff. %	DSC M+1=31	FEM N=230	Rel. Diff. %	DSC M+1=31	FEM N=230	Rel. Diff. %	DSC M+1=31	FEM N=230	Rel. Diff. %	DSC M+1=31	FEM N=230
1	9.573	9.535	0.399	10.861	11.356	-4.354	9.143	9.489	-3.642	10.024	10.402	-3.633	9.458	9.433	0.262	10.399	10.346	0.516
2	38.669	38.353	0.823	45.631	45.652	-0.047	38.444	38.320	0.323	41.867	41.844	0.055	38.285	37.959	0.859	41.581	41.438	0.345
3	86.644	86.254	0.453	102.727	102.719	0.008	86.774	86.259	0.597	94.406	94.175	0.245	85.774	85.367	0.477	93.386	93.219	0.179
4	153.716	153.292	0.277	182.618	182.611	0.004	153.786	153.283	0.328	167.607	167.395	0.126	152.158	151.713	0.293	165.883	165.705	0.107
5	239.916	239.474	0.184	285.337	285.329	0.003	239.960	239.453	0.212	261.745	261.536	0.080	237.470	237.007	0.195	259.082	258.899	0.070
6	345.253	344.805	0.130	410.883	410.873	0.002	345.277	344.768	0.148	376.803	376.596	0.055	341.722	341.250	0.138	372.986	372.802	0.049
7	469.733	469.283	0.096	559.254	559.244	0.002	469.736	469.230	0.108	512.780	512.576	0.040	464.917	464.444	0.102	507.597	507.413	0.036
8	613.357	612.911	0.073	730.452	730.441	0.001	613.339	612.838	0.082	669.677	669.476	0.030	607.059	606.589	0.077	662.915	662.734	0.027
9	776.127	775.688	0.057	924.475	924.464	0.001	776.085	775.593	0.063	847.492	847.296	0.023	768.149	767.686	0.060	838.941	838.763	0.021
10	958.043	957.614	0.045	1141.325	1141.313	0.001	957.977	957.496	0.050	1046.226	1046.035	0.018	948.187	947.735	0.048	1035.674	1035.502	0.017

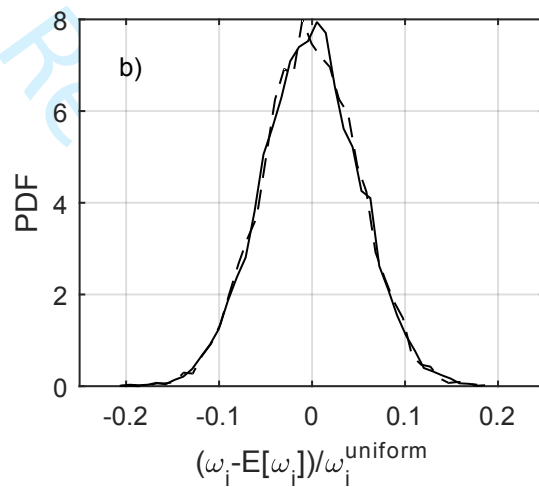
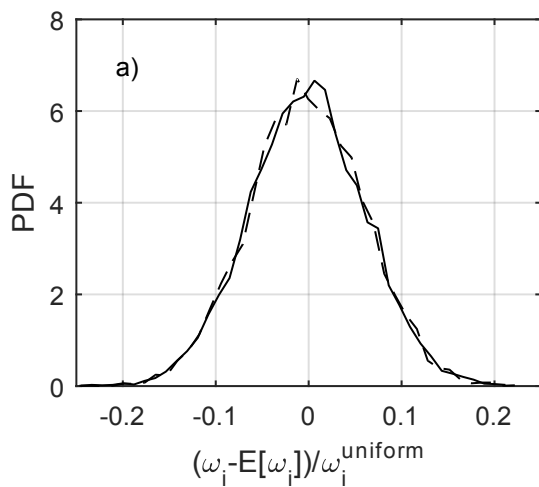
1  
2  
3 As inferred from Table 3, for different non-uniform structures, the DSC and FEM results are  
4 not exactly the same but are very consistent with each other. Average computational time is  
5  
6 2.87 s and 0.36 s for FEM and the DSC, respectively. Besides, the consistency of the methods  
7  
8 reduces for the more complex forms of Young's modulus and thickness. Considering both the  
9  
10 relative difference and the computational time, the DSC even with a very small number of  
11  
12 discretization points may represent non-uniform structures well and thus reliably used in  
13  
14 further complex structures.  
15  
16  
17  
18  
19  
20

### 21 **3.2. Stochastic analysis**

22  
23 In this part of the study, the effects of the geometrical and material variabilities on the natural  
24 frequencies are investigated using the DSC and PC expansion (DSC-PCE). In this manner, the  
25 beam thickness, Young's Modulus and specific volume vary globally with a normal  
26 distribution, i.e. they are uncertain variables but their distributions are known. In the analyses,  
27 the standard deviations of the uncertain variables are 5% of their mean values given in Table  
28 1. Seven uncertainty cases are considered for the uniform and non-uniform beams as shown in  
29 Table 4. The analysis starts by solving Eq. (21) eight times for the determination of each  
30 coefficient given in Eq. (19). Then, the distribution functions of the natural frequencies are  
31 determined using these coefficients with 10000 samples noting that  $\omega_n = \sqrt{\lambda_n}$ . In Fig. 4,  
32 probability distribution functions of the non-dimensional natural frequency ratio,  
33  $(\omega_i - E[\omega_i]) / \omega_i^{uniform}$ , are compared with those obtained by Monte Carlo (MC) simulations  
34 performed on the DSC models. Here  $E[\omega_i]$  denotes the mean value of the  $i$ th mode. Since  
35 each of the probability distribution functions of the non-dimensional natural frequency ratio is  
36 the same for all  $i=1,2, \dots,10$ , the probability distribution functions are represented here by a  
37 single figure. Note that, 10000 samples of uncertain variables are also used in MC  
38 simulations.  
39  
40  
41  
42  
43  
44  
45  
46  
47  
48  
49  
50  
51  
52  
53  
54  
55  
56  
57  
58  
59  
60

**Table 4. Uncertainty cases**

Non-uniformity	Form of the thickness, $h(x)$	Form of Young's modulus, $E(x)$	Uncertain parameters: $E(\vartheta_1)$ , $h(\vartheta_2)$ , $r(\vartheta_3)$
Uniform	$h_0$	$E$	Case 1
Non-uniform	$h_0(1+\beta x)^2$	$E$	Case 2
	$h_0$	$E \begin{pmatrix} 1+0.02 \cos(2\pi x/l) \\ +0.01 \sin(4\pi x/l) \end{pmatrix}$	Case 3
	$h_0(1+\beta x)^2$	$E \begin{pmatrix} 1+0.02 \cos(2\pi x/l) \\ +0.01 \sin(4\pi x/l) \end{pmatrix}$	Case 4
	$h_0(1+\beta x)$	$E \begin{pmatrix} 1+0.02 \cos(2\pi x/l) \\ +0.01 \sin(4\pi x/l) \end{pmatrix}$	Case 5
	$h_0(1+\beta x)^2$	$E(1-0.02x/l)^2$	Case 6
	$h_0(1+\beta x)$	$E(1-0.02x/l)^2$	Case 7



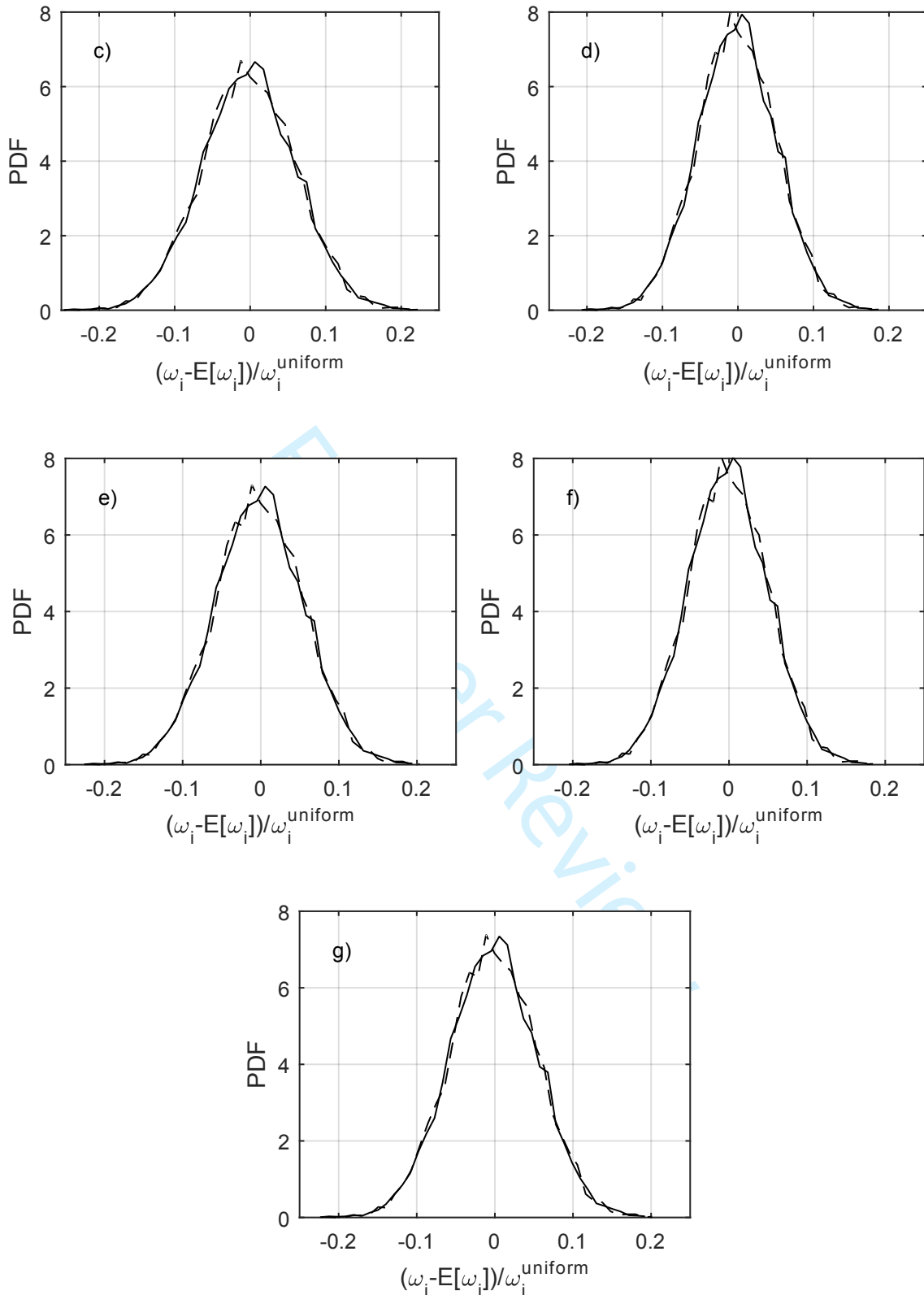


**Figure 4. Probability distribution functions of non-dimensional natural frequency ratios for uncertain a) Case 1, b) Case 2, c) Case 3, d) Case 4, e) Case 5, f) Case 6, g) Case 7 (solid line: PCE, dash line: Monte Carlo)**

1  
2  
3  
4  
5 It is seen from Fig. 4 that the predictions of the DSC-PCE are quite consistent with those of  
6 MC simulations for all cases. Besides, average computation time for the DSC-PCE is 3.72 s  
7  
8 whereas it is 8.52 for Monte Carlo simulation. The results show that DSC-PCE method is  
9  
10 very accurate and efficient and therefore can be reliably used for uncertainty analysis of non-  
11  
12 uniform structures.  
13  
14  
15  
16  
17  
18

#### 19 **4. Conclusions**

20  
21 In this study, a combination of Discrete Singular Convolution (DSC) and Polynomial  
22  
23 Chaos Expansion (PCE) is introduced for non-uniform beams having geometrical and  
24  
25 material variabilities. The DSC method is applied to model the non-uniform beam having  
26  
27 local changes in the Young's Modulus and thickness along its length. The PCE is utilized to  
28  
29 handle variabilities simulating uncertainty in a global manner. The DSC-PCE method is  
30  
31 verified for uniform and non-uniform beams using the finite element method and Monte Carlo  
32  
33 simulations. It is shown that the DSC method is very straightforward in modelling non-  
34  
35 uniformity along the spatial domain, and it is very accurate even with a relatively small  
36  
37 number of discretization points compared to the finite element method. It is also shown that  
38  
39 the combined DSC-PCE methodology is very efficient in computational cost and it quantifies  
40  
41 quite well the uncertainty due to the geometrical and material parameters. The study promises  
42  
43 that the present methodology is worth further development in order to apply it to more  
44  
45 complex systems, especially for mid and high frequency analysis.  
46  
47  
48  
49  
50  
51  
52  
53

#### 54 **Acknowledgments**

55  
56 This study is supported by "The Scientific and Technological  
57  
58 Research Council of Turkey, TUBITAK" in the frame of TUBITAK 2219.  
59  
60

### Declaration of Conflicting Interests

The Authors declare that there is no conflict of interest.

### References

- Akgöz B and Civalek Ö (2013) Longitudinal vibration analysis of strain gradient bars made of functionally graded materials (FGM). *Composites Part B: Engineering* 55. Elsevier: 263–268. DOI: 10.1016/j.compositesb.2013.06.035.
- Alshorbagy AE, Eltaher MA and Mahmoud FF (2011) Free vibration characteristics of a functionally graded beam by finite element method. *Applied Mathematical Modelling* 35(1). Elsevier: 412–425. DOI: 10.1016/j.apm.2010.07.006.
- Bailey CD (1978) Direct analytical solutions to non-uniform beam problems. *Journal of Sound and Vibration* 56(4). Academic Press: 501–507. DOI: 10.1016/0022-460X(78)90292-4.
- Baltacıoğlu AK, Akgöz B and Civalek Ö (2010) Nonlinear static response of laminated composite plates by discrete singular convolution method. *Composite Structures* 93(1): 153–161. DOI: 10.1016/j.compstruct.2010.06.005.
- Baltacıoğlu AK, Civalek Ö, Akgöz B, et al. (2011) Large deflection analysis of laminated composite plates resting on nonlinear elastic foundations by the method of discrete singular convolution. *International Journal of Pressure Vessels and Piping* 88(8–9): 290–300. DOI: 10.1016/j.ijpvp.2011.06.004.
- Civalek Ö (2007) Three-dimensional vibration, buckling and bending analyses of thick rectangular plates based on discrete singular convolution method. *International Journal of Mechanical Sciences* 49(6). Pergamon: 752–765. DOI: 10.1016/J.IJMECSCI.2006.10.002.
- Civalek Ö (2008a) Free vibration of curvilinear membranes by eight-noded Discrete Singular

1  
2  
3 Convolution (DSC). *International Journal of Science & Technology* 3(2): 165–171. DOI:  
4  
5 10.05.2008.  
6

7 Civalek Ö (2008b) Vibration analysis of membranes with arbitrary shapes using discrete  
8  
9 singular convolution. *CMES - Computer Modeling in Engineering and Sciences* 31(1):  
10  
11 25–36. DOI: 10.1525/sp.2007.54.1.23.  
12  
13

14 Civalek Ö (2009) Eigenvalues of membranes having skew and rhombic geometry using  
15  
16 discrete singular convolution algorithm. *Communications in Nonlinear Science and*  
17  
18 *Numerical Simulation* 14(11). Elsevier: 4003–4009. DOI: 10.1016/j.cnsns.2008.08.010.  
19  
20

21 Civalek Ö (2013) Nonlinear dynamic response of laminated plates resting on nonlinear elastic  
22  
23 foundations by the discrete singular convolution-differential quadrature coupled  
24  
25 approaches. *Composites Part B: Engineering* 50: 171–179. DOI:  
26  
27 10.1016/j.compositesb.2013.01.027.  
28  
29

30 Civalek Ö (2017) Free vibration of carbon nanotubes reinforced (CNTR) and functionally  
31  
32 graded shells and plates based on FSDT via discrete singular convolution method.  
33  
34 *Composites Part B: Engineering* 111: 45–59. DOI: 10.1016/j.compositesb.2016.11.030.  
35  
36

37 Elishakoff I and Johnson V (2005) Apparently the first closed-form solution of vibrating  
38  
39 inhomogeneous beam with a tip mass. *Journal of Sound and Vibration* 286(4–5).  
40  
41 Academic Press: 1057–1066. DOI: 10.1016/j.jsv.2005.01.050.  
42  
43

44 Ersoy H, Özpolat L and Civalek Ö (2009) Free vibration of circular and annular membranes  
45  
46 with varying density by the method of discrete singular convolution. *Structural*  
47  
48 *Engineering and Mechanics* 32(5). Techno-Press: 621–634. DOI:  
49  
50 10.12989/sem.2009.32.5.621.  
51  
52

53 Ersoy H, Civalek Ö and Özpolat L (2010) Free vibration analysis of rectangular membranes  
54  
55 with variable density using the discrete singular convolution approach. *Asian Journal of*  
56  
57 *Civil Engineering (Building And Housing)* 11(1): 83–94.  
58  
59  
60



- 1  
2  
3 Evans DH (1972) An application of numerical integration techniques to statistical tolerancing,  
4  
5 III—general distributions. *Technometrics* 14(1). Taylor & Francis Group: 23–35. DOI:  
6  
7 10.1080/00401706.1972.10488880.  
8  
9
- 10 Evans M and Swartz T (2000) *Approximating Integrals via Monte Carlo and Deterministic*  
11  
12 *Methods*. Oxford: Oxford University Press.  
13  
14
- 15 Falsone G and Impollonia N (2004) About the accuracy of a novel response surface method  
16  
17 for the analysis of finite element modeled uncertain structures. In: *Probabilistic*  
18  
19 *Engineering Mechanics*, 1 January 2004, pp. 53–63. Elsevier. DOI:  
20  
21 10.1016/j.pro bengmech.2003.11.005.  
22  
23
- 24 Ghanem RG and Spanos PD (2003) *Stochastic Finite Elements: A Spectral Approach*. New  
25  
26 York: Dover Publications.  
27  
28
- 29 Gürses M, Civalek Ö, Korkmaz AK, et al. (2009) Free vibration analysis of symmetric  
30  
31 laminated skew plates by discrete singular convolution technique based on first-order  
32  
33 shear deformation theory. *International Journal for Numerical Methods in Engineering*  
34  
35 79(3). John Wiley & Sons, Ltd: 290–313. DOI: 10.1002/nme.2553.  
36  
37
- 38 Gürses M, Akgöz B and Civalek Ö (2012) Mathematical modeling of vibration problem of  
39  
40 nano-sized annular sector plates using the nonlocal continuum theory via eight-node  
41  
42 discrete singular convolution transformation. *Applied Mathematics and Computation*  
43  
44 219(6): 3226–3240. DOI: 10.1016/j.amc.2012.09.062.  
45  
46
- 47 Hohenbichler M and Rackwitz R (1989) Improvement of second-order reliability estimates by  
48  
49 importance sampling. *Journal of Engineering Mechanics* 114(12): 2195–2199. DOI:  
50  
51 10.1061/(ASCE)0733-9399(1988)114:12(2195).  
52  
53
- 54 Impollonia N and Sofi A (2003) A response surface approach for the static analysis of  
55  
56 stochastic structures with geometrical nonlinearities. *Computer Methods in Applied*  
57  
58 *Mechanics and Engineering* 192(37–38). Elsevier: 4109–4129. DOI: 10.1016/S0045-  
59  
60

1  
2  
3 7825(03)00379-7.  
4

5 Kara M and Seçgin A (2019) Discrete singular convolution method for one-dimensional  
6 vibration and acoustics problems with impedance boundaries. *Journal of Sound and*  
7 *Vibration* 446. Academic Press: 22–36. DOI: 10.1016/j.jsv.2019.01.028.  
8  
9

10 Keane AJ and Price WC (1997) *Statistical Energy Analysis. An Overview with Applications in*  
11 *Structural Dynamics*. Keane A and Price W (eds). Cambridge: Cambridge University  
12 Press.  
13  
14  
15  
16

17 Kompella MS and Bernhard RJ (1993) Measurement of the statistical variation of structural-  
18 acoustic characteristics of automotive vehicles. In: *SAE Technical Papers*, 1993. SAE  
19 International. DOI: 10.4271/931272.  
20  
21  
22

23 Korayem MH and Homayooni A (2017) The size-dependent analysis of multilayer micro-  
24 cantilever plate with piezoelectric layer incorporated voltage effect based on a modified  
25 couple stress theory. *European Journal of Mechanics, A/Solids* 61. Elsevier Ltd: 59–72.  
26  
27  
28  
29  
30  
31  
32  
33  
34  
35  
36

37 Korayem MH, Sadeghzadeh S and Rahneshin V (2012) A new multiscale methodology for  
38 modeling of single and multi-body solid structures. *Computational Materials Science* 63.  
39 Elsevier: 1–11. DOI: 10.1016/j.commat.2012.05.059.  
40  
41

42 Lucor D, Su CH and Karniadakis GE (2004) Generalized polynomial chaos and random  
43 oscillators. *International Journal for Numerical Methods in Engineering* 60(3). Wiley-  
44 Blackwell: 571–596. DOI: 10.1002/nme.976.  
45  
46  
47  
48

49 Mercan K and Civalek Ö (2016) DSC method for buckling analysis of boron nitride nanotube  
50 (BNNT) surrounded by an elastic matrix. *Composite Structures* 143. Elsevier: 300–309.  
51  
52  
53  
54  
55  
56

57 Nazemizadeh M and Bakhtiari-Nejad F (2015) A general formulation of quality factor for  
58 composite micro/nano beams in the air environment based on the nonlocal elasticity  
59  
60

theory. *Composite Structures* 132. Elsevier Ltd: 772–783. DOI:

10.1016/j.compstruct.2015.05.070.

Rahman S and Xu H (2004) A univariate dimension-reduction method for multi-dimensional integration in stochastic mechanics. *Probabilistic Engineering Mechanics* 19(4): 393–408. DOI: 10.1016/j.probengmech.2004.04.003.

Rao SS (2011) *Mechanical Vibrations*. 5th Ed. New York: Prentice Hall.

Rubinstein RY and Kroese DP (2016) *Simulation and the Monte Carlo Method*. John Wiley & Sons.

Sankar B V. (2001) An elasticity solution for functionally graded beams. *Composites Science and Technology* 61(5). Elsevier: 689–696. DOI: 10.1016/S0266-3538(01)00007-0.

Seçgin A (2013) Modal and response bound predictions of uncertain rectangular composite plates based on an extreme value model. *Journal of Sound and Vibration* 332(5): 1306–1323. DOI: 10.1016/j.jsv.2012.09.036.

Seçgin A and Kara M (2018) Vibration bounding of uncertain thin beams by using an extreme value model based on statistical moments. *JVC/Journal of Vibration and Control* 24(23). SAGE Publications Sage UK: London, England: 5627–5641. DOI: 10.1177/1077546318763203.

Seçgin A and Sarigül AS (2008) Free vibration analysis of symmetrically laminated thin composite plates by using discrete singular convolution (DSC) approach: Algorithm and verification. *Journal of Sound and Vibration* 315(1–2). Academic Press: 197–211. DOI: 10.1016/j.jsv.2008.01.061.

Seçgin A and Sarigül AS (2009) A novel scheme for the discrete prediction of high-frequency vibration response: Discrete singular convolution–mode superposition approach. *Journal of Sound and Vibration* 320(4–5). Academic Press: 1004–1022. DOI: 10.1016/j.jsv.2008.08.031.

- 1  
2  
3 Seçgin A, Dunne JF and Zoghaib L (2012) Extreme-value-based statistical bounding of low,  
4 mid, and high frequency responses of a forced plate with random boundary conditions.  
5  
6 *Journal of Vibration and Acoustics* 134(2). American Society of Mechanical Engineers:  
7  
8 021003. DOI: 10.1115/1.4005019.  
9  
10  
11  
12 Seo HS and Kwak BM (2002) Efficient statistical tolerance analysis for general distributions  
13 using three-point information. *International Journal of Production Research* 40(4).  
14  
15 Taylor & Francis Group: 931–944. DOI: 10.1080/00207540110095709.  
16  
17  
18  
19 Sepahvand K (2017) Stochastic finite element method for random harmonic analysis of  
20 composite plates with uncertain modal damping parameters. *Journal of Sound and*  
21  
22 *Vibration* 400: 1–12. DOI: 10.1016/j.jsv.2017.04.025.  
23  
24  
25  
26 Sepahvand K, Marburg S and Hardtke H-J (2007) Numerical solution of one-dimensional  
27 wave equation with stochastic parameters using generalized polynomial chaos  
28  
29 expansion. *Journal of Computational Acoustics* 15(04): 579–593. DOI:  
30  
31 10.1142/S0218396X07003524.  
32  
33  
34  
35 Sepahvand K, Marburg S and Hardtke H-J (2010) Uncertainty quantification in stochastic  
36 systems using polynomial chaos expansion. *International Journal of Applied Mechanics*  
37  
38 02(02): 305–353. DOI: 10.1142/S1758825110000524.  
39  
40  
41  
42 Shokrollahi M and Zayeri Baghlani Nejad A (2014) Numerical analysis of free longitudinal  
43 vibration of nonuniform rods: Discrete Singular Convolution approach. *Journal of*  
44  
45 *Engineering Mechanics* 140(8): 06014007. DOI: 10.1061/(ASCE)EM.1943-  
46  
47 7889.0000772.  
48  
49  
50  
51 Tan G, Wang W and Jiao Y (2016) Flexural free vibrations of multistep nonuniform beams.  
52  
53 *Mathematical Problems in Engineering* 2016. Hindawi: 1–12. DOI:  
54  
55 10.1155/2016/7314280.  
56  
57  
58 Tan G, Liu Y, Gong Y, et al. (2018) Free Vibration of the Cracked Non-uniform Beam with  
59  
60

- 1  
2  
3 Cross Section Varying as Polynomial Functions. *KSCE Journal of Civil Engineering*  
4  
5 22(11). Springer Verlag: 4530–4546. DOI: 10.1007/s12205-018-1833-5.  
6  
7  
8 Wei GW (1999) Discrete singular convolution for the solution of the Fokker–Planck equation.  
9  
10 *The Journal of Chemical Physics* 110(18): 8930–8942. DOI: 10.1063/1.478812.  
11  
12 Wei GW (2001a) A new algorithm for solving some mechanical problems. *Computer*  
13  
14 *Methods in Applied Mechanics and Engineering* 190(15–17): 2017–2030. DOI:  
15  
16 10.1016/S0045-7825(00)00219-X.  
17  
18 Wei GW (2001b) Discrete singular convolution for beam analysis. *Engineering Structures*  
19  
20 23(9): 1045–1053. DOI: 10.1016/S0141-0296(01)00016-5.  
21  
22 Wei GW (2001c) Vibration analysis by discrete singular convolution. *Journal of Sound and*  
23  
24 *Vibration* 244(3): 535–553. DOI: 10.1006/jsvi.2000.3507.  
25  
26  
27 Wei GW, Zhao YB and Xiang Y (2001) The determination of natural frequencies of  
28  
29 rectangular plates with mixed boundary conditions by discrete singular convolution.  
30  
31 *International Journal of Mechanical Sciences* 43(8). Pergamon: 1731–1746. DOI:  
32  
33 10.1016/S0020-7403(01)00021-2.  
34  
35  
36 Wei GW, Zhao YB and Xiang Y (2002a) A novel approach for the analysis of high-frequency  
37  
38 vibrations. *Journal of Sound and Vibration* 257(2): 207–246. DOI: 10.1006/jsvi.5055.  
39  
40  
41 Wei GW, Zhao YB and Xiang Y (2002b) Discrete singular convolution and its application to  
42  
43 the analysis of plates with internal supports. Part 1: Theory and algorithm. *International*  
44  
45 *Journal for Numerical Methods in Engineering* 55(8). John Wiley & Sons, Ltd.: 913–  
46  
47 946. DOI: 10.1002/nme.526.  
48  
49  
50 Zhao S, Wei GW and Xiang Y (2005) DSC analysis of free-edged beams by an iteratively  
51  
52 matched boundary method. *Journal of Sound and Vibration* 284(1–2): 487–493. DOI:  
53  
54 10.1016/j.jsv.2004.08.037.  
55  
56  
57  
58  
59  
60

**Table 1. Material and geometrical properties of the beam**

<b>Property (<i>Unit</i>)</b>	<b>Value</b>
Young's modulus (Pa)	3.25E+10
Density (kgm <sup>-3</sup> )	2500
Thickness at $x=0$ (m)	0.25
Width (m)	0.3
Length (m)	15

For Peer Review

**Table 2. Natural frequencies of the simply supported uniform beam (rad/s)**

Mode Seq.	Analy. (Rao, 2011)	DSC N=11	DSC N=21	DSC N=31	FEM N=20	FEM N=60	FEM N=120	FEM N=230
1	11.414	11.411	11.414	11.414	11.414	11.414	11.414	11.414
2	45.656	45.667	45.656	45.656	45.656	45.656	45.656	45.656
3	102.726	102.828	102.726	102.726	102.730	102.726	102.726	102.726
4	182.624	183.501	182.624	182.624	182.644	182.624	182.624	182.624
5	285.350	290.841	285.350	285.350	285.424	285.351	285.350	285.350
6	410.904	434.686	410.904	410.904	411.124	410.907	410.905	410.904
7	559.287	627.888	559.287	559.287	559.835	559.294	559.287	559.287
8	730.497	858.099	730.497	730.497	731.707	730.512	730.498	730.497
9	924.535	1059.665	924.538	924.535	926.960	924.566	924.537	924.535
10	1141.401		1141.427	1141.401	1145.906	1141.460	1141.405	1141.401
<b>Error %</b>								
1	-	-2.78E-02	-3.55E-05	-4.39E-07	4.22E-05	4.92E-07	2.80E-06	8.27E-06
2	-	2.35E-02	2.16E-06	2.71E-08	6.75E-04	8.35E-06	5.94E-07	1.01E-06
3	-	9.94E-02	-4.05E-07	-5.27E-09	3.40E-03	4.22E-05	2.70E-06	5.67E-07
4	-	4.80E-01	1.20E-07	1.62E-09	1.07E-02	1.33E-04	8.36E-06	8.20E-07
5	-	1.92E+00	-2.74E-08	-6.42E-10	2.60E-02	3.26E-04	2.04E-05	1.61E-06
6	-	5.79E+00	2.57E-07	2.98E-10	5.34E-02	6.75E-04	4.22E-05	3.14E-06
7	-	1.23E+01	3.01E-06	-1.51E-10	9.81E-02	1.25E-03	7.83E-05	5.82E-06
8	-	1.75E+01	3.26E-05	8.31E-11	1.66E-01	2.13E-03	1.33E-04	9.90E-06
9	-	1.46E+01	2.97E-04	-4.72E-11	2.62E-01	3.40E-03	2.14E-04	1.59E-05
10	-		2.24E-03	2.80E-11	3.95E-01	5.18E-03	3.26E-04	2.42E-05

1  
2  
3  
4  
5  
6  
7  
8  
9  
10  
11  
12  
13  
14  
15  
16  
17  
18  
19  
20  
21  
22  
23  
24  
25  
26  
27  
28  
29  
30  
31  
32  
33  
34  
35  
36  
37  
38  
39  
40  
41  
42  
43  
44  
45  
46

**Table 3. Natural frequencies of the simply supported non-uniform beam (rad/s)**

Form of thickness and Young's modulus	$h(x) = h_0(1 + \beta x)^2$ $E(x) = E$			$h(x) = h_0$ $E(x) = E \begin{pmatrix} 1 + 0.02 \cos(2\pi x/l) \\ + 0.01 \sin(4\pi x/l) \end{pmatrix}$			$h(x) = h_0(1 + \beta x)^2$ $E(x) = E \begin{pmatrix} 1 + 0.02 \cos(2\pi x/l) \\ + 0.01 \sin(4\pi x/l) \end{pmatrix}$			$h(x) = h_0(1 + \beta x)$ $E(x) = E \begin{pmatrix} 1 + 0.02 \cos(2\pi x/l) \\ + 0.01 \sin(4\pi x/l) \end{pmatrix}$			$h(x) = h_0(1 + \beta x)^2$ $E(x) = E(1 - 0.02x/l)^2$			$h(x) = h_0(1 + \beta x)$ $E(x) = E(1 - 0.02x/l)^2$		
	Mode Seq.	DSC M+1=31	FEM N=230	Rel. Diff. %	DSC M+1=31	FEM N=230	Rel. Diff. %	DSC M+1=31	FEM N=230	Rel. Diff. %	DSC M+1=31	FEM N=230	Rel. Diff. %	DSC M+1=31	FEM N=230	Rel. Diff. %	DSC M+1=31	FEM N=230
1	9.573	9.535	0.399	10.861	11.356	-4.354	9.143	9.489	-3.642	10.024	10.402	-3.633	9.458	9.433	0.262	10.399	10.346	0.516
2	38.669	38.353	0.823	45.631	45.652	-0.047	38.444	38.320	0.323	41.867	41.844	0.055	38.285	37.959	0.859	41.581	41.438	0.345
3	86.644	86.254	0.453	102.727	102.719	0.008	86.774	86.259	0.597	94.406	94.175	0.245	85.774	85.367	0.477	93.386	93.219	0.179
4	153.716	153.292	0.277	182.618	182.611	0.004	153.786	153.283	0.328	167.607	167.395	0.126	152.158	151.713	0.293	165.883	165.705	0.107
5	239.916	239.474	0.184	285.337	285.329	0.003	239.960	239.453	0.212	261.745	261.536	0.080	237.470	237.007	0.195	259.082	258.899	0.070
6	345.253	344.805	0.130	410.883	410.873	0.002	345.277	344.768	0.148	376.803	376.596	0.055	341.722	341.250	0.138	372.986	372.802	0.049
7	469.733	469.283	0.096	559.254	559.244	0.002	469.736	469.230	0.108	512.780	512.576	0.040	464.917	464.444	0.102	507.597	507.413	0.036
8	613.357	612.911	0.073	730.452	730.441	0.001	613.339	612.838	0.082	669.677	669.476	0.030	607.059	606.589	0.077	662.915	662.734	0.027
9	776.127	775.688	0.057	924.475	924.464	0.001	776.085	775.593	0.063	847.492	847.296	0.023	768.149	767.686	0.060	838.941	838.763	0.021
10	958.043	957.614	0.045	1141.325	1141.313	0.001	957.977	957.496	0.050	1046.226	1046.035	0.018	948.187	947.735	0.048	1035.674	1035.502	0.017



**Table 4. Uncertainty cases**

<b>Non-uniformity</b>	<b>Form of the thickness, <math>h(x)</math></b>	<b>Form of Young's modulus, <math>E(x)</math></b>	<b>Uncertain parameters: <math>E(\vartheta_1)</math>, <math>h(\vartheta_2)</math>, <math>r(\vartheta_3)</math></b>
<b>Uniform</b>	$h_0$	$E$	Case 1
<b>Non-uniform</b>	$h_0(1 + \beta x)^2$	$E$	Case 2
	$h_0$	$E \begin{pmatrix} 1 + 0.02 \cos(2\pi x/l) \\ + 0.01 \sin(4\pi x/l) \end{pmatrix}$	Case 3
	$h_0(1 + \beta x)^2$	$E \begin{pmatrix} 1 + 0.02 \cos(2\pi x/l) \\ + 0.01 \sin(4\pi x/l) \end{pmatrix}$	Case 4
	$h_0(1 + \beta x)$	$E \begin{pmatrix} 1 + 0.02 \cos(2\pi x/l) \\ + 0.01 \sin(4\pi x/l) \end{pmatrix}$	Case 5
	$h_0(1 + \beta x)^2$	$E(1 - 0.02 x/l)^2$	Case 6
	$h_0(1 + \beta x)$	$E(1 - 0.02 x/l)^2$	Case 7

1  
2  
3  
4  
5  
6  
7  
8  
9  
10  
11  
12  
13  
14  
15  
16  
17  
18  
19  
20  
21  
22  
23  
24  
25  
26  
27  
28  
29  
30  
31  
32  
33  
34  
35  
36  
37  
38  
39  
40  
41  
42  
43  
44  
45  
46  
47  
48  
49  
50  
51  
52  
53  
54  
55  
56  
57  
58  
59  
60

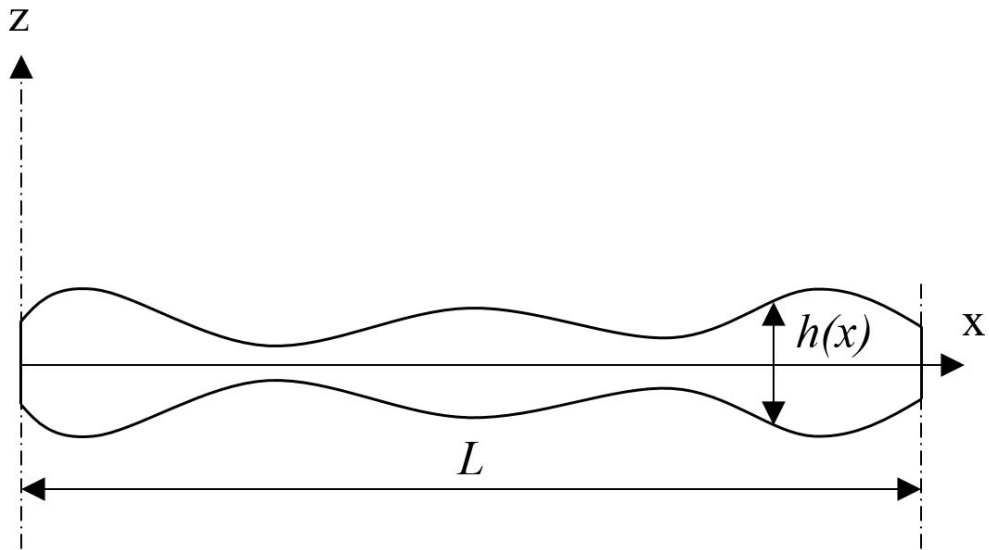
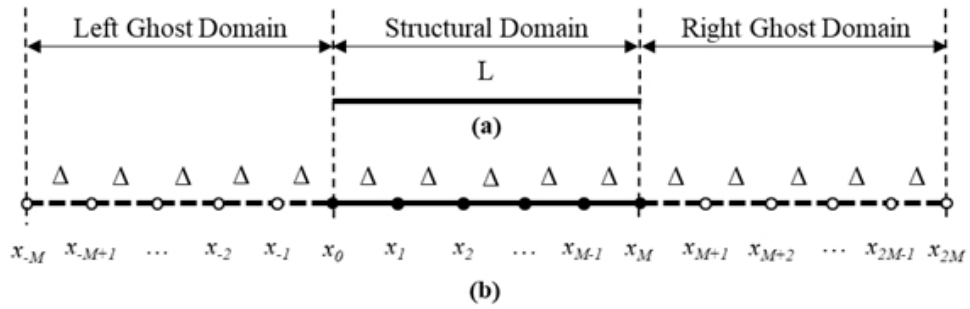


Figure 1. A beam structure with its geometrical parameters

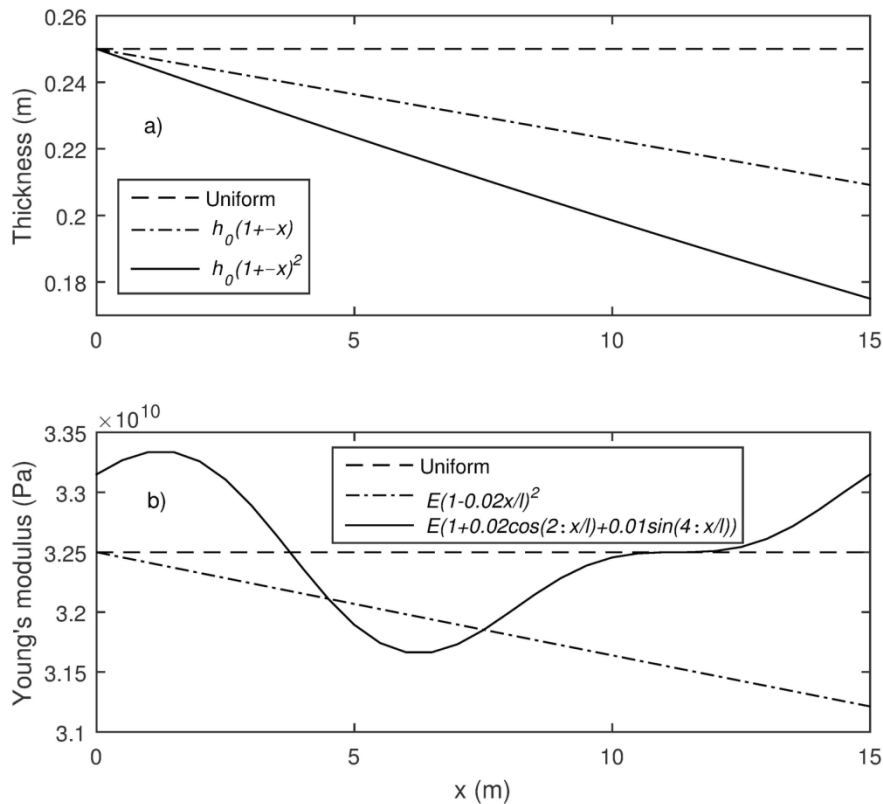
285x157mm (96 x 96 DPI)



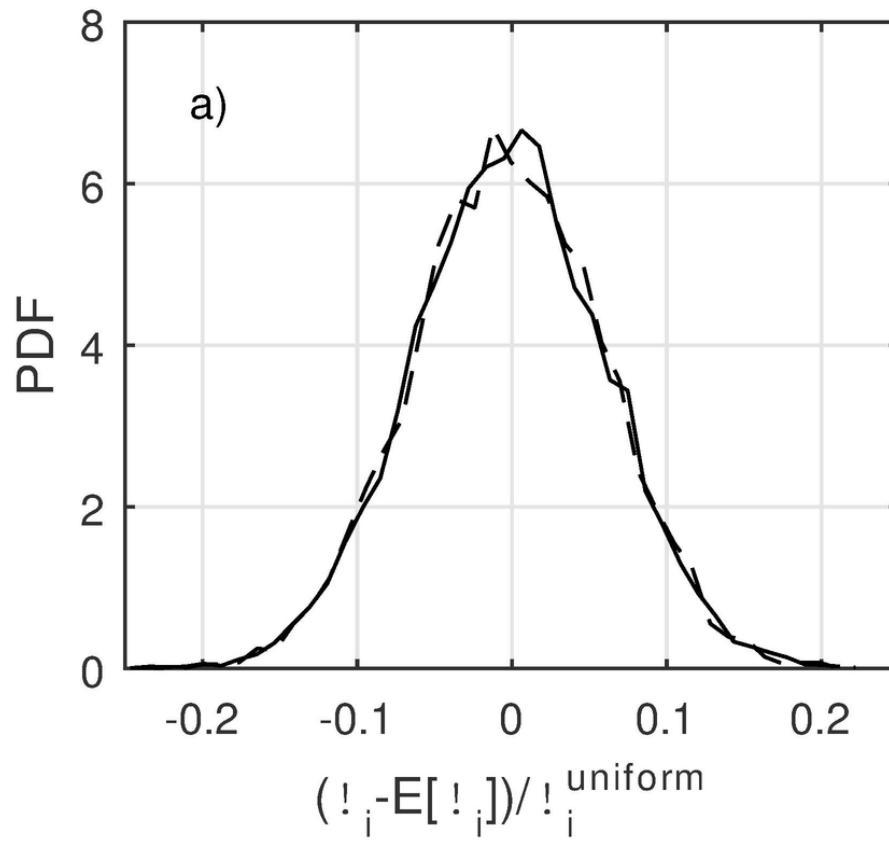
**Figure 2**

156x60mm (96 x 96 DPI)

1  
2  
3  
4  
5  
6  
7  
8  
9  
10  
11  
12  
13  
14  
15  
16  
17  
18  
19  
20  
21  
22  
23  
24  
25  
26  
27  
28  
29  
30  
31  
32  
33  
34  
35  
36  
37  
38  
39  
40  
41  
42  
43  
44  
45  
46  
47  
48  
49  
50  
51  
52  
53  
54  
55  
56  
57  
58  
59  
60

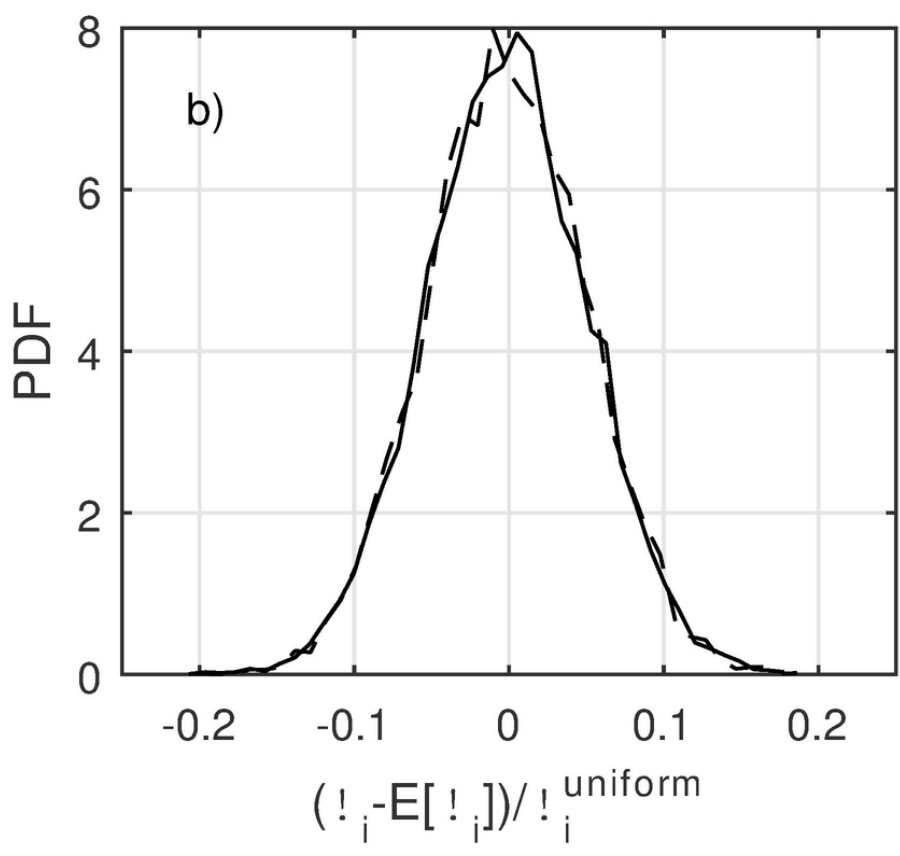


157x138mm (300 x 300 DPI)

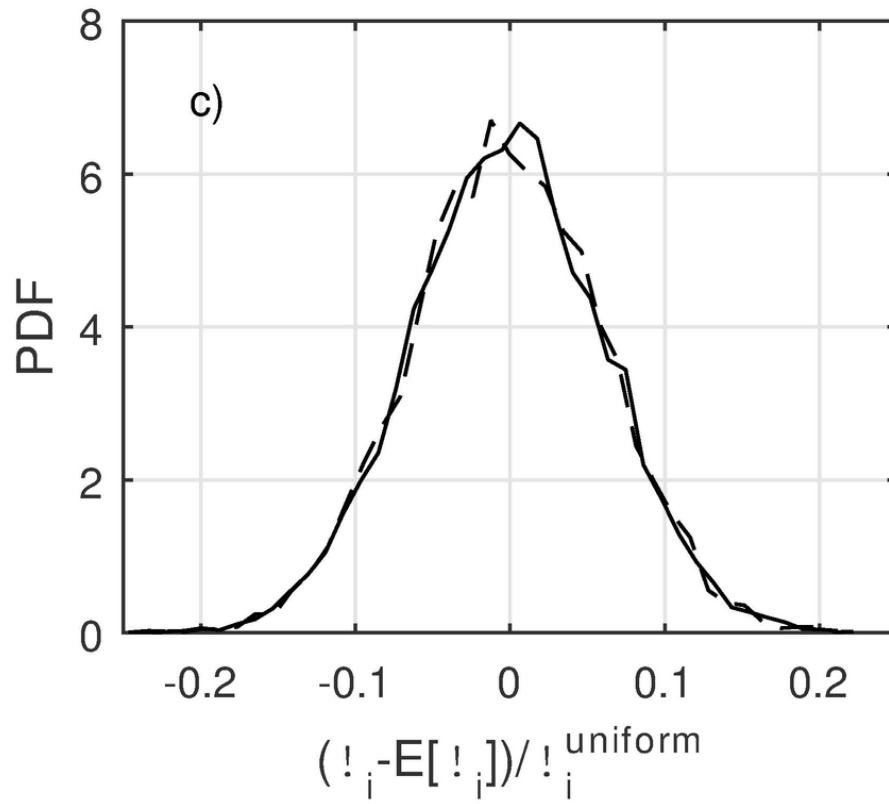


78x70mm (300 x 300 DPI)

1  
2  
3  
4  
5  
6  
7  
8  
9  
10  
11  
12  
13  
14  
15  
16  
17  
18  
19  
20  
21  
22  
23  
24  
25  
26  
27  
28  
29  
30  
31  
32  
33  
34  
35  
36  
37  
38  
39  
40  
41  
42  
43  
44  
45  
46  
47  
48  
49  
50  
51  
52  
53  
54  
55  
56  
57  
58  
59  
60

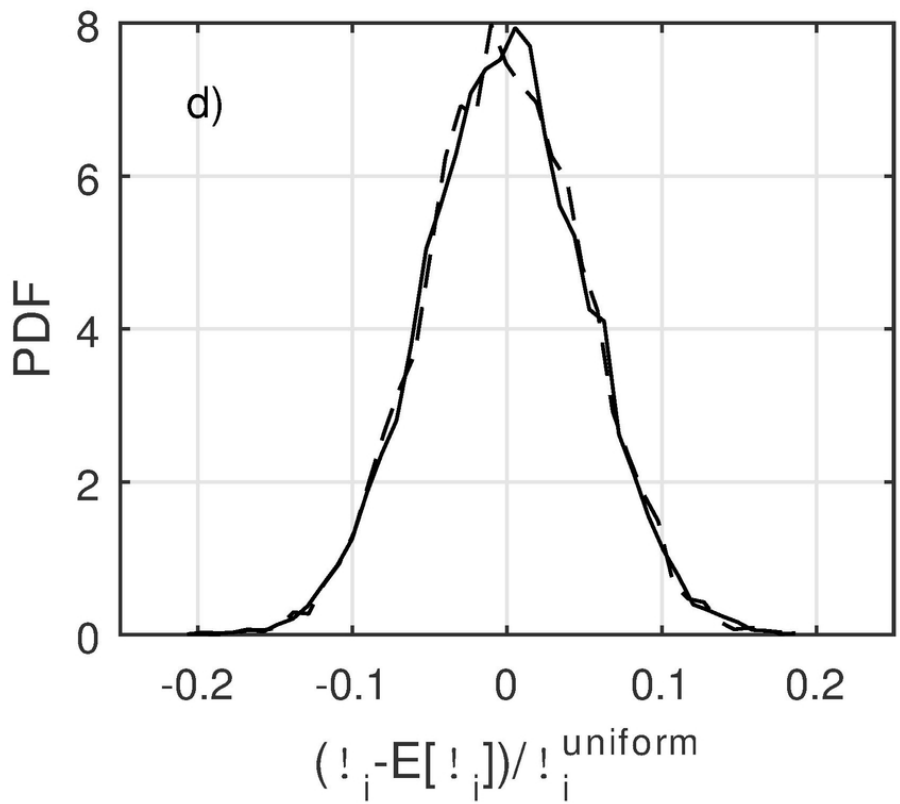


78x70mm (300 x 300 DPI)



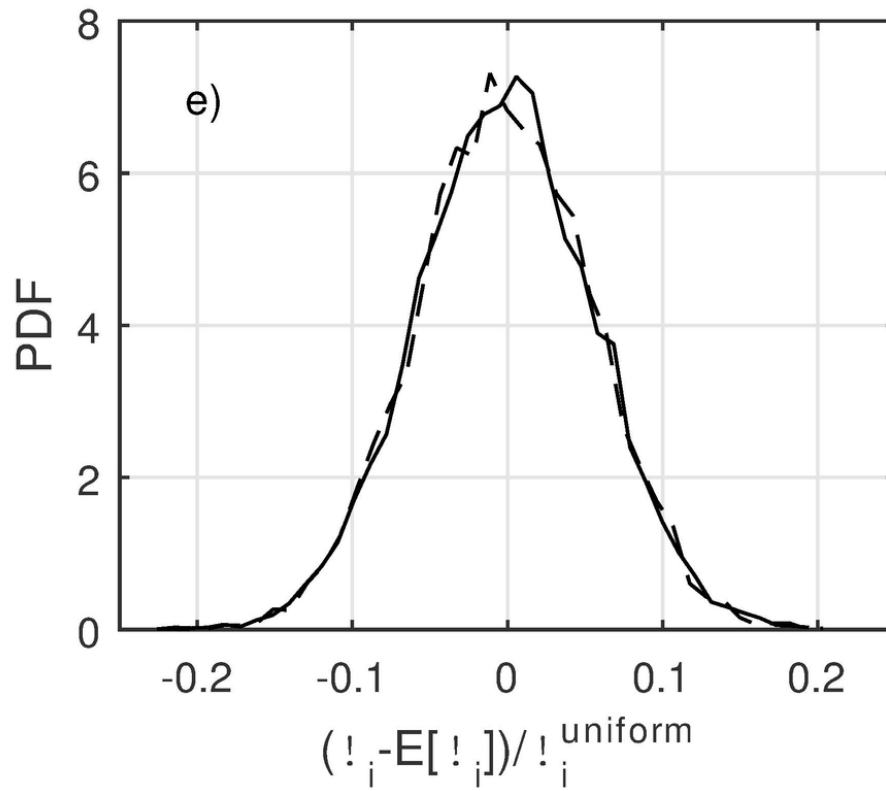
79x67mm (300 x 300 DPI)

1  
2  
3  
4  
5  
6  
7  
8  
9  
10  
11  
12  
13  
14  
15  
16  
17  
18  
19  
20  
21  
22  
23  
24  
25  
26  
27  
28  
29  
30  
31  
32  
33  
34  
35  
36  
37  
38  
39  
40  
41  
42  
43  
44  
45  
46  
47  
48  
49  
50  
51  
52  
53  
54  
55  
56  
57  
58  
59  
60

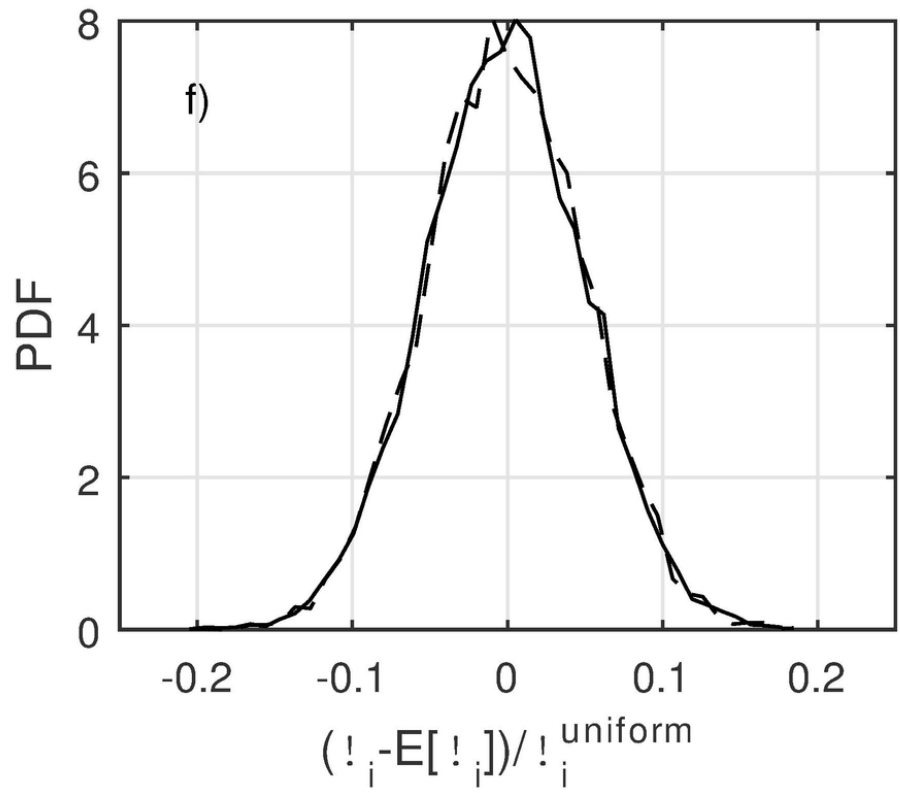


79x67mm (300 x 300 DPI)

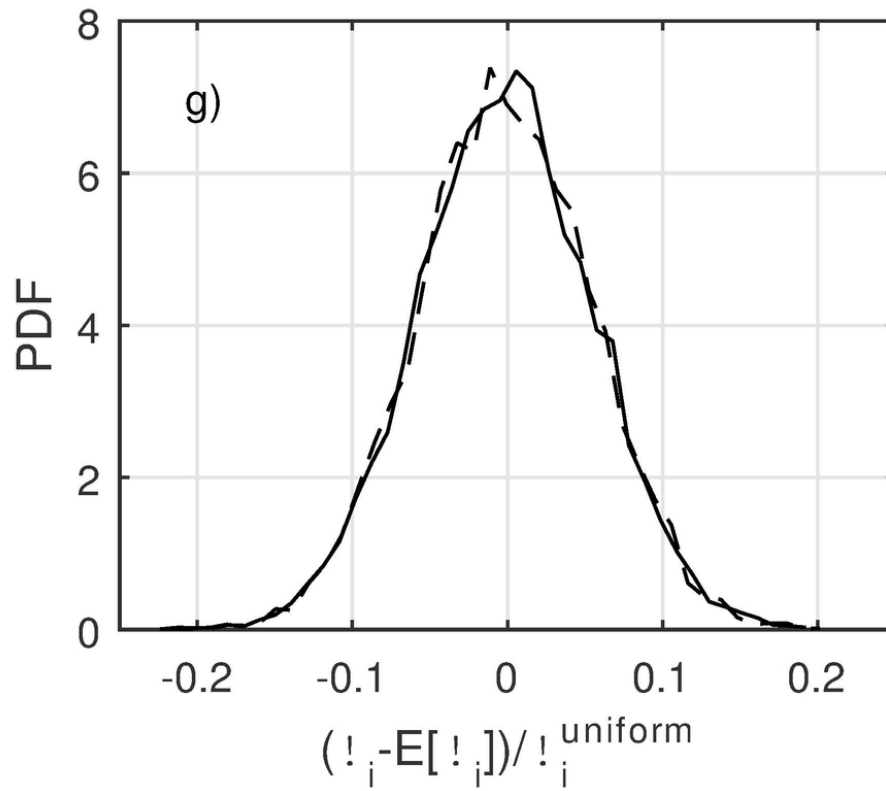




1  
2  
3  
4  
5  
6  
7  
8  
9  
10  
11  
12  
13  
14  
15  
16  
17  
18  
19  
20  
21  
22  
23  
24  
25  
26  
27  
28  
29  
30  
31  
32  
33  
34  
35  
36  
37  
38  
39  
40  
41  
42  
43  
44  
45  
46  
47  
48  
49  
50  
51  
52  
53  
54  
55  
56  
57  
58  
59  
60



82x68mm (300 x 300 DPI)



82x68mm (300 x 300 DPI)